Journal of Catalysis 436 (2024) 115583

Contents lists available at ScienceDirect

Journal of Catalysis

journal homepage: www.elsevier.com/locate/jcat

The role of chlorine promoters in mediating particle size effects in silver-catalyzed ethylene epoxidation

Krishna R. Iyer, Aditya Bhan *

Department of Chemical Engineering and Materials Science, University of Minnesota, Minneapolis, MN 55455, USA

ARTICLE INFO

Keywords:
Ethylene epoxidation
Chlorine
Particle size
Silver

ABSTRACT

Measured chlorine coverages over Ag/α-Al_2O_3 catalysts with varying Ag weight loadings (1.3–35 wt%) and different Ag particle size distributions when parsed in terms of Cl coverages over particles of varying size constituted in the distribution reveal that Ag particles of size below ~30 nm are covered in more than 1 monolayer (ML) of chlorine in presence of 3.5 ppm C_2H_5Cl. These assessments of Cl coverages were made possible by correlating the cumulative Cl coverage to the lognormal surface area distribution of 22 Ag/α-Al_2O_3 samples using a single exponential decay function. Fully chlorided small Ag particles exhibit low rates of epoxidation and only large Ag particles which exhibit sub-monolayer Cl coverages catalyze ethylene epoxidation with high ethylene oxide (EO) rates and selectivity. The Ag particle size dependence of Cl coverages plausibly explains why ≥ 100 nm Ag particles are typical in promoted Ag/α-Al_2O_3 ethylene epoxidation catalysts.

1. Introduction

Silver-catalyzed ethylene epoxidation is a large-scale selective oxidation chemistry [1] that relies on the unique ability of large Ag clusters to activate molecular O_2 [2]. High selectivity (~90%) to the desired product, ethylene oxide (EO), over promoted Ag/α-Al_2O_3 catalysts is enabled by a continuous cofeed of ppm levels of organochloride promoters (primarily ethyl chloride or vinyl chloride) that deposit chlorine adatoms on the catalyst surface [3,4]. Typical Ag weight loadings for Ag/α-Al_2O_3 catalyst formulations are ~35 wt% [5,6]; these formulations contain large Ag clusters that expose 0.5–1% of Ag atoms on the surface because large silver particles (~100–150 nm) have been found to exhibit high EO rates and high EO selectivity [7]. The large Ag particle sizes of ethylene epoxidation catalysts defy conventional arguments based on structural factors like specific geometric configuration of atoms [8] or electronic effects related to binding energy of an adsorbate [9] to nanometer-sized metal clusters [10] or charge transfer between metal and the support [10,11] that are typically associated with sub-10 nm metal clusters [12]. A key parameter known to systematically influence ethylene epoxidation rates and ethylene oxide selectivity over silver single crystal [8] and promoted Ag/α-Al_2O_3 catalysts [3] is the chlorine coverage. We inquire whether variations in EO rates and EO selectivity with Ag particle size can be explained by changes in the chlorine coverage with particle size. We address this question by correlating measured Cl coverages with the silver particle size distribution over 9 Ag/α-Al_2O_3 catalysts with Ag weight loadings ranging from 1.3 to 35 wt% at varying chloriding conditions (1.5 to 8 ppm C_2H_5Cl). The key finding from this model is that small silver particles are covered in multiple monolayers of chlorine at 1.5–8 ppm ethyl chloride promoter concentrations in the gas phase that are typical of ethylene epoxidation catalysis leading to low epoxidation rates on these small Ag particles. Only when large Ag particles (>100 nm) are present and organochloride promoter concentrations are carefully moderated [3,5,13] can ethylene epoxidation catalysis be enabled at high EO rates and high EO selectivity.

2. Materials and methods

2.1. Catalyst synthesis and characterization

The procedure to synthesize Ag/α-Al_2O_3 catalysts by incipient-wetness impregnation of $Ag_2C_2O_4$ over α-Al_2O_3 was described in detail in a previous publication [7]. Briefly, 1.5 g of oxalic acid (Fisher Scientific, 99.6 %) and 2.04 g silver nitrate (Thermo Scientific, 99.7 %) were added to 50 cm^3 of deionized water at ambient temperature and stirred for 10 min resulting in the formation of a white precipitate (silver oxalate, $Ag_2C_2O_4$) that was then washed in deionized water and vacuum filtered for ~ 12 h at ambient temperature. The α-Al_2O_3 support was

* Corresponding author.
E-mail addresses: iyer0040@umn.edu (K.R. Iyer), abhan@umn.edu (A. Bhan).

https://doi.org/10.1016/j.jcat.2024.115583
Received 30 November 2023; Received in revised form 7 April 2024; Accepted 1 June 2024
Available online 2 June 2024

impregnated with a solution containing $Ag_2C_2O_4$ dissolved in a mixture of 1:1 vol ratio of water: ethylene diamine (Sigma-Aldrich, Reagent Plus, >99 %) followed by drying in static air at 333 K. The deposited $Ag_2C_2O_4$ was treated in 0.83 $cm^3\ s^{-1}$ He for 2 h at 498 K to decompose the Ag precursor to form Ag/α-Al_2O_3. The molarity of $Ag_2C_2O_4$ solution was varied between 0.07 M to 2.5 M to obtain Ag/α-Al_2O_3 formulations with different Ag weight loadings varying between 1.3 wt% and 35 wt% as characterized using Scanning Electron Microscopy with energy dispersive X-ray spectroscopy (SEM-EDX) analysis. The Ag/α-Al_2O_3 formulations were treated in different gas atmospheres (He (Matheson, Research grade), zero-grade air, H_2 (Airgas, UHP 99.999 %), and O_2 (Matheson, 99.9 %)) at different gas flowrates and temperatures as detailed in Table 1. Ag nanoparticle sizes were measured after reaction by Scanning Electron Microscopy (SEM, Hitachi SU8230 Field emission gun, 5 or 10 kV electron beam accelerating voltage). The spent catalyst was prepared for SEM imaging by coating it on a thin film of amorphous carbon. Three SEM images representing different regions over the catalyst and ~1600 Ag particles were analyzed for each catalyst sample using ImageJ to evaluate the Ag particle size distribution. Ag particles were approximated to be perfect hemispheres and their diameters are referred to as size. This assumption limits assessment of whether rates are dependent of different Ag facets [14] and whether edge or corner sites play a role in catalysis. The sampling error introduced by approximating the total population of silver particles using a sample of size ~1600 was quantified to be less than 2% (Supporting Information Section S.1). A summary of the total surface area per gram, the surface area weighted particle diameter ($D_{S.A.}$), and silver dispersion determined after reaction, calculated using Eqs. 1–3, for the 9 Ag/α-Al_2O_3 formulations used as catalysts is given in Table 1.

$$\text{Total surface area per gram } (m^2 g_{Ag}^{-1}) = \frac{\sum_{i=1}^{n} 2\pi\left(\frac{s_i}{2}\right)^2}{\sum_{i=1}^{n} \frac{2\pi}{3}\left(\frac{s_i}{2}\right)^3 * \rho_{Ag}} \quad (1)$$

$$\text{Surface} - \text{area} - \text{weighted particle diameter } (D_{S.A.}) = \frac{6 * \sum_{i=1}^{n} \frac{2\pi}{3}\left(\frac{s_i}{2}\right)^3}{\sum_{i=1}^{n} 2\pi\left(\frac{s_i}{2}\right)^2} \quad (2)$$

$$\text{Ag dispersion} = \frac{\rho_{Ag_{surf}} * \sum_{i=1}^{n} 2\pi\left(\frac{s_i}{2}\right)^2}{\rho_{Ag} * \sum_{i=1}^{n} \frac{2\pi}{3}\left(\frac{s_i}{2}\right)^3} \quad (3)$$

where: s_i is the diameter of particle 'i', n is the total number of particles, $\rho_{Ag_{surf}}$ is the surface silver density, and ρ_{Ag} is the silver bulk density.

2.2. Measurement of ethylene epoxidation rates

Ethylene epoxidation rates were assessed in a stainless-steel packed-bed reactor (McMaster-Carr, OD = 6.36 mm, ID = 4.57 mm) with 20–100 mg of Ag/α-Al_2O_3 catalyst supported between two plugs of quartz wool (CE Elantech). The reactor was embedded between two split-tube copper sleeves and heated by two cartridge heaters (Omega Engineering Inc., CIR-2100, 600 W) to the reaction temperature (513 K) using a Watlow temperature controller (96 Series) and a K-type thermocouple (Omega Engineering Inc.) placed in the center of the catalyst bed with pressure maintained at 530 kPa using a backpressure regulator (Tescom). The reactor feed comprised of 30 mol% C_2H_4 (Airgas 99.99%), 0.17–0.4 mol% C_2H_6 (Matheson 10% diluted in He), 7.7 mol% O_2 (Matheson 99.99%), 1.5–8 ppm C_2H_5Cl (Airgas 160 ppm diluted in He), and 1 mol% CO_2 (Matheson 10% diluted in He), and the respective gases were supplied to the reactor through mass flow controllers (MKS G-series) at a total flowrate of 2.78 $cm^3\ s^{-1}$. The measured EO rates were free from external heat and mass-transfer limitations as confirmed by calculations using GradientCheck [15] as reported in Supporting Information Section S.2. The reactor effluent flowed through a 0.5 cm^3 stainless steel sample loop which was injected into a gas chromatograph (GC, Agilent 7890A) equipped with an HP-Plot Q column (30 m × 320 μm × 20 μm) and a thermal conductivity detector (TCD) in series with a flame ionization detector (FID) before discharging the effluent into a bubbler containing 0.5 M H_2SO_4 (BeanTown Chemical). The gas lines upstream of the reactor were heated to 393 K using heat tapes (W.W. Grainger) to prevent condensation of the effluent gas stream. The catalyst typically restructures under reaction conditions [16] thus it was exposed to the reaction mixture for ~18 h on stream wherein during the last 10 h on stream, no significant changes were observed either in EO rates or EO selectivity as shown in Figure S.5 of a prior publication [7]. Thus, EO rates at 18 h on stream are reported as the catalyst reaches a steady state rate by averaging rates enumerated from 3 GC injections.

Table 1
Surface area weighted particle diameter ($D_{S.A.}$), total surface area per gram, and silver dispersion for different Ag/α-Al_2O_3 samples. These observables change depending on the C_2H_5Cl chloride concentration in the feed (1.5–8 ppm); the data tabulated are recorded for samples after reaction. The Ag weight loading of the sample has been mentioned as a prefix in the sample name. All samples were initially treated in 1.25 $cm^3\ s^{-1}$ flowing He at 498 K with a ramp rate of 0.17 K s^{-1} and dwell time of 2 h. The suffix label for each sample corresponds to a specific heat treatment post synthesis detailed in the footnote. Reaction conditions: 30 mol% C_2H_4, 7.7 mol% O_2, 1 mol% CO_2, 1.5–8 ppm C_2H_5Cl, 0.17–0.4 mol% C_2H_6, balance He; 5.3 bar; 513 K; catalyst mass = 0.02–0.1 g of unpromoted 1.3–35 wt% Ag/α-Al_2O_3 and the C_2H_5Cl concentration used is specified in the column header. Histograms depicting the surface area per gram as a function of particle size for all samples are shown in Supporting Information Section S.10.

Sample name	$D_{S.A.}$ / nm			Total area per gram / $m^2_{Ag} g^{-1}_{Ag}$			Silver dispersion / %		
	C_2H_5Cl concentration / ppm								
	1.5	3.5	8	1.5	3.5	8	1.5	3.5	8
1.3S-1	80.4 ± 23.4	64 ± 20.6	55.2 ± 18.0	7.1	8.6	10.1	1.80	2.24	2.62
2.2S-1	64.1 ± 20.6	66.5 ± 20.9	64.1 ± 20.7	8.9	7.5	8.9	2.23	2.25	2.22
6.9S-1	82.3 ± 27.2	73.1 ± 23.4	84.3 ± 25.6	6.8	7.6	6.9	1.74	2.07	1.71
9.9S-2	97.2 ± 31.5	80 ± 25.4	82.9 ± 26.9	5.8	6.4	7.0	1.49	1.73	2.13
16.9S-2	107.2 ± 35.6	93.6 ± 31.5	92.7 ± 30.0	5.3	5.4	5.6	1.34	1.37	1.57
35S-2	201.4 ± 67.5	176.1 ± 54.1	163.7 ± 58.2	2.8	3.2	3.4	0.75	0.81	0.89
35S-3	264 ± 87.2	261.6 ± 82.6	255 ± 91.9	2.1	2.1	2.2	0.49	0.51	0.56
35S-4	–	203 ± 70.3	–	–	2.4	–	–	0.71	–
35S-5	–	272 ± 89.3	–		2.1	–	–	0.59	–

Heat treatment conditions:
S-1—1.25 $cm^3\ s^{-1}$ H_2, ramp at 0.17 K s^{-1}, hold at 498 K for 2 h.
S-2 – no further heat treatment.
S-3—0.83 $cm^3\ s^{-1}$ air, ramp at 0.17 K s^{-1}, hold at 598 K for 4 h.
S-4—0.83 $cm^3\ s^{-1}$ O_2, ramp at 0.17 K s^{-1}, hold at 848 K for 4 h.
S-5—0.83 $cm^3\ s^{-1}$ He, ramp at 0.17 K s^{-1}, hold at 943 K for 4 h.

Ethylene conversions varied between 0.1–1% and oxygen conversions were less than 6%, and the carbon mole balance (total carbon moles in/total carbon moles out) closed within 2.5%. Product selectivities (S_j) reported in the study are defined as moles of carbon in the product divided by moles of carbon in all products (Eqs. (4)–(5)).

$$r_j = \frac{(F_{out} - F_{in})_j}{m_{cat}} \quad (4)$$

$$S_j = \frac{r_j n_j}{\sum r_j n_j} x\,100 \quad (5)$$

Where: $(F_{out})_j$, $(F_{in})_j$ are molar flowrate of product "j", m_{cat} is the mass of catalyst, r_j is the rate of product "j', n_j is the number of C atoms in product "j".

2.3. Measurement of chlorine coverage in a recycle reactor

The chlorine coverage was measured over the catalyst after reaction in an external recycle reactor with high recycle ratio (>20) to enumerate chlorine content of the sample by flowing 0.1 $cm^3\ s^{-1}$ of a mixture of 5 mol% ethane and 2.5 mol% oxygen. Molecules with weak C–H homolytic bond enthalpies such as ethane have been shown to remove chlorine from the Ag surface [17]. Most of the chlorine (>95 %) is removed in a single such experiment in the form of ethyl chloride as seen in Fig. 1. The area under the curve in Fig. 1 can be integrated to find the total chlorine content of the catalyst. Chlorine coverage was then calculated as the moles of chlorine divided by the moles of surface silver (Eq. (3) shows how Ag dispersion was calculated).

A control experiment was done to determine whether chlorine could be taken up by the α-Al_2O_3 support. In this experiment the α-Al_2O_3 support was exposed to 15 ppm C_2H_5Cl in presence of O_2 at 513 K and atmospheric pressure and thereafter the sample was exposed to C_2H_6/O_2 mixtures following protocols similar to the ones described above. No Cl* uptake was noted on the α-Al_2O_3 support (Supporting Information Section S.11).

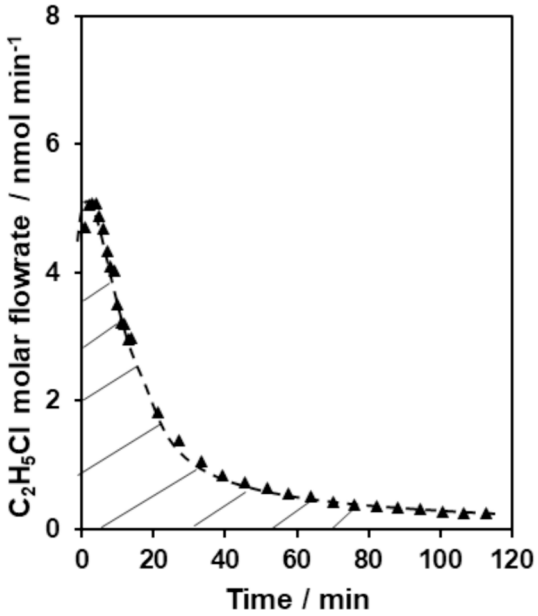

Fig. 1. Molar flowrate of ethyl chloride measured as a function of time in a recycle flow reactor. Reaction conditions: 30 mol% C_2H_4, 7.7 mol% O_2, 1 mol% CO_2, 8 ppm C_2H_5Cl, 0.17 mol% C_2H_6, balance He; 5.3 bar; 513 K; catalyst mass = 0.04 g unpromoted 35 wt% Ag/α-Al_2O_3; followed by chlorine counting in a recycle reactor using 0.1 $cm^3\ s^{-1}$ of 5 mol% C_2H_6, 2.5 mol% O_2 mixture at 513 K and 110 kPa. Dashed line is a guide to the eye.

3. Results and discussion

3.1. Effect of promoter chlorine on the Ag particle size distribution

Ag/α-Al_2O_3 catalysts have been noted previously to undergo structural changes upon exposure to reactive gas environments leading to broadening of the Ag particle size distribution compared to the as-synthesized sample [7]. The distribution of exposed Ag surface area as a function of particle size of all post-reaction Ag/α-Al_2O_3 catalyst samples can be represented as a lognormal distribution as shown in Supporting Information Section S.10. The silver dispersion of 7 Ag/α-Al_2O_3 catalysts determined after reaction by examining ~1600 Ag particles using SEM increased with increasing ethyl chloride concentration in the feedstream (Supporting Information Figure S.2) suggesting that chlorine helps redisperse Ag particles. The fractional surface area exposed by particles <40 nm over a 1.3 wt% Ag/α-Al_2O_3 catalyst increased from 0.27 to 0.35 as the ethyl chloride concentration was increased from 1.5 ppm to 8 ppm (Fig. 2) resembling the increase in the fraction of <100 nm particles from 47% to 70% post reaction over an as-synthesized 10 wt% Ag/α-Al_2O_3 catalyst in presence of 1 ppm vinyl chloride at 20 bar and 498 K observed by van Hoof et al. [18] Redispersal of Ag particles from an average size of 172 nm for an 8.2 wt% Ag/α-Al_2O_3 catalyst on-stream for 60 h to an average size of 127 nm upon addition of 1 ppm vinyl chloride to the reaction mixture (5 mol% C_2H_4, 10 mol% O_2, 498 K, 20 bar) also evidences that chlorine induces changes in the size of Ag clusters [16]. An underlying and unanswered question is whether chlorine is uniformly distributed over these clusters of different sizes.

3.2. Ethylene epoxidation rates and selectivity as a function of average particle size at different chlorinating conditions

EO rates measured at different chlorinating conditions over 7 different Ag/α-Al_2O_3 catalysts with weight loadings ranging from 1.3-35 wt% are shown in Fig. 3 (a). EO rates increase with increasing average particle size up to a certain size before starting to decrease with Ag particle size at all ethyl chloride concentrations tested. The optimum average particle size that maximizes the EO rate changes depending on the concentration of ethyl chloride in the feedstream. Catalysts with low

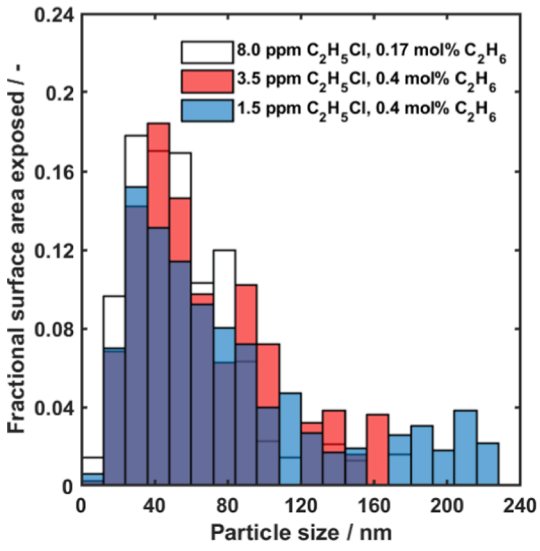

Fig. 2. Fractional surface area exposed by Ag particles of different sizes over a 1.3 wt% Ag/α-Al_2O_3 sample exposed to different chloriding conditions during ethylene epoxidation. Reaction conditions: 30 mol% C_2H_4, 7.7 mol% O_2, 1 mol % CO_2, 1.5–8 ppm C_2H_5Cl, 0.17–0.4 mol% C_2H_6, balance He; 5.3 bar; 513 K; catalyst mass = 0.05–0.092 g unpromoted 1.3 wt% Ag/α-Al_2O_3, ethylene conversions ranging from 0.01 to 0.03 % and EO selectivities ranging from 41 and 63 %.

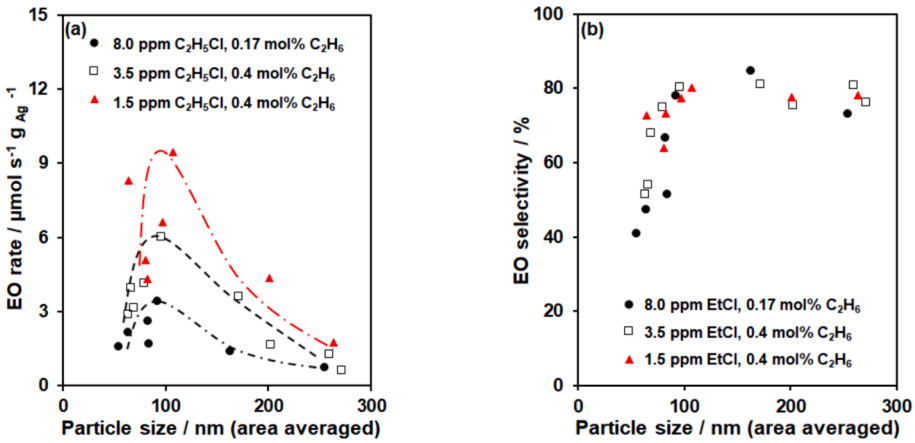

Fig. 3. (a) EO rates (b) EO selectivity measured as a function of surface area averaged particle size at different chloriding conditions. Reaction conditions: 30 mol% C_2H_4, 7.7 mol% O_2, 1 mol% CO_2, 1.5–8 ppm C_2H_5Cl, 0.17–0.4 mol% C_2H_6, balance He; 5.3 bar; 513 K; catalyst mass = 0.02–0.1 g unpromoted 1.3–35 wt% Ag/α-Al_2O_3. Each datapoint was acquired at 18 h on-stream after steady state rates were obtained. Dashed lines are a guide to the eye.

average particle size have low EO selectivity (Fig. 3 (b)) whereas, particle size has little effect on EO selectivity for large Ag particles (>100 nm).

Chlorine coverage was assessed over these catalysts after reaction by feeding 0.1 $cm^3\ s^{-1}$ of 5 mol% C_2H_6 and 2.5 mol% O_2 in an external recycle flow reactor (CSTR) by measuring the flowrate of C_2H_5Cl formed upon removal of Cl by C_2H_6 over time, the area under the curve was integrated (Fig. 1) to find the total chlorine content of the catalyst. Chlorine coverage was then calculated as the moles of chlorine divided by the moles of surface silver (silver dispersion reported in Table 1). At identical process conditions, the 1.3 wt% Ag/α-Al_2O_3 sample with the lowest average size exhibits the highest chlorine coverage (Fig. 4 (a)). Notably, chlorine coverage increases from 45% at 3.5 ppm C_2H_5Cl to 75% at 8 ppm C_2H_5Cl over the 1.3 wt% Ag/α-Al_2O_3 highlighting that Cl coverages depend sensitively on the chlorinating conditions. The chlorine coverages measured over different catalysts can be replotted as a function of surface area averaged particle size as shown in Fig. 4 (b). Chlorine coverage decreases with average silver particle size before becoming nearly invariant with average size which was verified by measuring chlorine coverages at 3.5 ppm C_2H_5Cl over two additional 35 wt% Ag samples with average diameter >200 nm (labelled as 35S-4 and 35S-5 in Fig. 4 (b)). Although trends based on average particle size suggest a sensitive dependence of chlorine coverages on the Ag particle size, a functional relationship between chlorine coverage and particle size can be established only by correlating particle size distributions with coverages. Catalysts with similar average size (~64–66 nm) highlighted in Fig. 4 (b) have chlorine coverages ranging from 15 % to 45 % at 3.5 ppm C_2H_5Cl and 0.4 mol% ethane in the feed, thus average size is incomplete as a descriptor in relation to chlorine coverage. Instead, we posit that chlorine coverage for different sized Ag particles within the distribution must be disambiguated to develop a more complete description of particle size effects in ethylene epoxidation catalysis.

Additional context for particle-size-dependent chlorine coverages being relevant in ethylene epoxidation catalysis is provided by re-examining the trends in EO selectivity with average particle size (Fig. 3 (b)) based on measured chlorine coverages. Chlorine coverage is known to improve EO selectivity over promoted Ag/α-Al_2O_3 catalysts [4,19] as observed over the 35 wt% Ag/α-Al_2O_3 sample with a large average particle size (Supporting Information Figure S.3). However, over the low Ag weight loading samples (1.3, 2.2 wt% Ag) with small average particle sizes (<100 nm), EO selectivity appears to be inversely correlated with chlorine coverage (Supporting Information Section S.4). This disparity among samples with large- and small- average Ag particle size can be explained by examining how chlorine coverage changes with

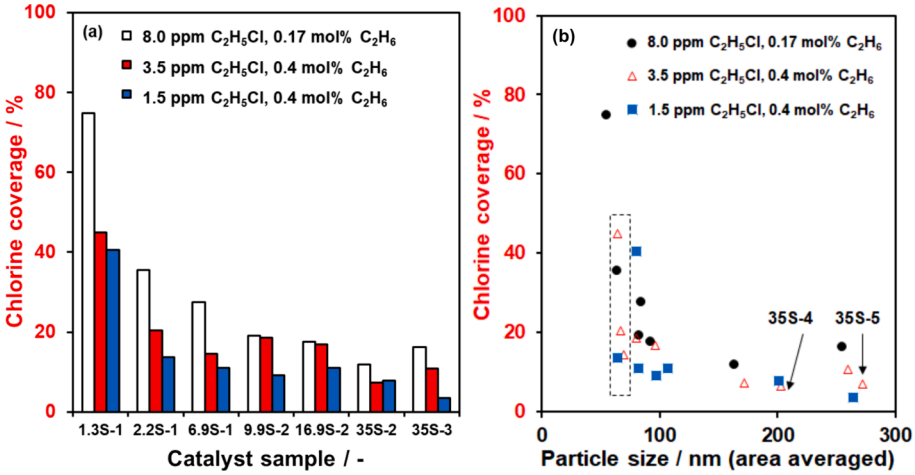

Fig. 4. (a) Chlorine coverage measured at different chloriding conditions over Ag/α-Al_2O_3 catalysts with varying Ag loadings (1.3–35 wt%) subjected to different post synthetic heat treatment conditions (Catalyst nomenclature detailed in Table 1). (b) Chlorine coverage measured as a function of surface area averaged particle size for different Ag/α-Al_2O_3 catalysts. Reaction conditions: 30 mol% C_2H_4, 7.7 mol% O_2, 1 mol% CO_2, 1.5–8 ppm C_2H_5Cl, 0.17–0.4 mol% C_2H_6, balance He; 5.3 bar; 513 K; catalyst mass = 0.02–0.1 g unpromoted 1.3–35 wt% Ag/α-Al_2O_3; followed by chlorine counting in a recycle reactor using 0.1 $cm^3\ s^{-1}$ of 5 mol% C_2H_6, 2.5 mol % O_2 mixture at 513 K and 110 kPa. Dashed rectangular area includes all catalyst samples with similar average particle size.

Ag particle size.

3.3. Chlorine coverage as a function of Ag particle size

Ag/α-Al_2O_3 catalysts exhibit a broad distribution of particle sizes under reaction conditions (Supporting Information Section S.10), and the measured chlorine content (T_{Cl}) of the catalyst is a cumulative quantity reflecting the sum of chlorine adsorbed over all Ag particles comprising the distribution. In an effort to determine chlorine coverages over Ag particles of varying size, we formulate a model (Eq. (6)), wherein the chlorine content (T_{Cl}) is defined as an integral of the product of two terms: (i) a chlorine-coverage dependent function F(s) that gives the chlorine content per unit surface area for a particle of size 's' and (ii) the surface area exposed per gram A(s) of particles of size 's' represented by a lognormal distribution (Eq. (8)).

$$T_{Cl}\ (\mu mol_{Cl}\ g_{Ag}^{-1}) = \int_{R_{min}}^{R_{max}} F(s) \times A(s)\, ds \tag{6}$$

$$F(s)\ (\mu mol_{Cl}\ m_{Ag}^{-2}) = ae^{-bs} + c \tag{7}$$

$$A(s)\ (m_{Ag}^2\ g_{Ag}^{-1}) = \frac{A}{(\text{bin size})\sigma\sqrt{2\pi s}} e^{-\frac{(\log(\frac{s}{\mu}))^2}{2*\sigma^2}} \tag{8}$$

The cumulative chlorine content was enumerated for each of the 7 catalyst samples (2 additional samples at 3.5 ppm C_2H_5Cl) across different process conditions (1.5, 3.5, 8 ppm C_2H_5Cl). The surface area distribution A(s) term, represented by a lognormal distribution as in Eq. (8), was determined using SEM of post-reaction samples as shown in Supporting Information Section S.10. Subsequently, these datasets at each chlorinating condition were fitted to Eq. (6) using Athena Visual Studio with various functional forms of F(s). An exponential function for F(s) shown in Eq. (7) fitted the experimental data across a wide range of particle sizes and chlorinating conditions as shown in Figure S.4 except for the 1.3 wt% Ag/α-Al_2O_3 at 8 ppm C_2H_5Cl which was an outlier (Supporting Information Section S.5). An exponential function for F(s) was chosen simply based on its ability to describe the observed chlorine coverage dependency on particle size as reported in Section 3.2. The fitted chlorine function F(s) can be divided by the areal atomic density of the Ag surface calculated by considering that it contains an equal fraction of Ag(1 1 1), Ag(1 1 0), and Ag(1 0 0) crystal facets to obtain the chlorine coverage as a function of particle size. The model predicts that the mole ratio of Cl to bulk Ag (calculated by multiplying the chlorine coverage by silver dispersion) exceeds 1 for certain small particle sizes which is physically infeasible (Figure S.6). Consequently, we restricted the maximum mole ratio of Cl to bulk Ag to 1, giving rise to a constraint (Eq. (10)) detailed in Section S.7 with the updated model equation shown in Eq. (9).

$$F(s) = F_{max}(s)e^{-b\times s} + c(1 - e^{-b\times s}) \tag{9}$$

$$F_{max}(s) = 23.29s \tag{10}$$

where the constraint in Eq. (10) ensures that the mole ratio of Cl to bulk Ag is below 1 at every particle size "s". A parity plot showing the close agreement between the experimentally measured chlorine content and that predicted by the model (Eqs. (9) and (10) over 7 Ag/α-Al_2O_3 samples at 3 different chlorinating conditions (two additional samples at 3.5 ppm C_2H_5Cl also reported) is shown in Fig. 5 (a).

Chlorine coverage calculated as a function of particle size as per the updated model (Eqs. 9–10) is shown in Fig. 5 (b). At 3.5 ppm C_2H_5Cl, particles below 28 nm are covered in >1 monolayer of chlorine. Less than 4% of the total mass of silver in any of the Ag/α-Al_2O_3 samples is covered in >1 ML chlorine as shown in Section S.9. van Hoof et al. [16,18] have noted previously that Ag restructures upon addition of organochloride promoters. The nature of Ag facets exposed has also been reported to impact ethylene epoxidation rates and selectivity [14]. However, no functional or mechanistic relationship between Ag particle size or topology and chlorine coverages has been reported for supported Ag olefin epoxidation catalysts. Affirming whether a monolayer coverage exists on small Ag particles is challenging given that these particles may not have a bulk stoichiometry of AgCl. Advanced characterization studies involving electron diffraction and identical location imaging TEM may help affirm these postulates in future studies. Excess chlorine likely diffuses into the bulk as indicated previously in ultra-high vacuum single crystal studies [20]. The strong affinity of small particles to adsorb chlorine strongly is akin to their tendency to adsorb oxygen strongly in comparison to large particles as indicated previously by thermal desorption studies of dioxygen [21] and by reactive molecular dynamics simulations [22]. Ethylene epoxidation rates can be completely poisoned over silver catalysts at high gas phase dichloroethane concentrations [23] likely due to high Cl coverages. This plausibly explains why small Ag particles have low EO rates in presence of 1.5–8 ppm organochloride promoter concentrations typical of EO

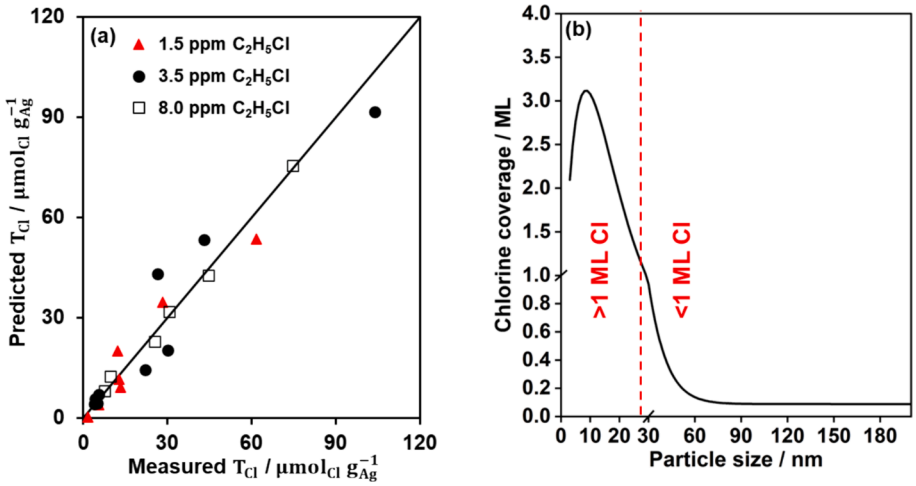

Fig. 5. (a) Parity plot comparing the measured chlorine content with values predicted by the updated exponential F_{max} model (Eqs. 9–10). Reaction conditions: 30 mol% C_2H_4, 7.7 mol% O_2, 1 mol% CO_2, 1.5–8 ppm C_2H_5Cl, 0.17–0.4 mol% C_2H_6, balance He; 5.3 bar; 513 K; catalyst mass = 0.02–0.1 g unpromoted 1.3–35 wt% Ag/α-Al_2O_3; followed by chlorine counting in a recycle reactor using 0.1 $cm^3\ s^{-1}$ of 5 mol% C_2H_6, 2.5 mol% O_2 mixture at 513 K and 110 kPa. (b) Chlorine coverage as a function of particle size as predicted by the model Eq. (9) at the following process conditions: 30 mol% C_2H_4, 7.7 mol% O_2, 1 mol% CO_2, 3.5 ppm C_2H_5Cl, 0.4 mol% C_2H_6, balance He; 5.3 bar; 513 K.

catalysis [7] as these particles are likely fully covered in chlorine. The model predicts sub-monolayer chlorine coverages for particles larger than 28 nm that decrease monotonically with size up to a silver particle size of 100 nm and thereafter become invariant with size (Fig. 5 (b)). In prior studies over promoted Ag/Al_2O_3 catalysts, it has been demonstrated that the optimal enhancement in EO rate occurs at low chlorine coverages, approximately 0.1 ML [3,4], similar to the coverage predicted by the model (Fig. 5 (b)) over large particles (>100 nm) which could account for the high EO rates observed over 100–150 nm Ag particles [7]. The invariance of chlorine coverage with size over large Ag particles explains why EO selectivity is unchanged with particle size above 100 nm (Fig. 3 (b)). While the chlorine coverage constitutes a prominent parameter contributing to particle size effects in ethylene epoxidation catalysis, prior investigations [9,10,24] have demonstrated variations in parameters such as oxygen binding energies implying that electronic characteristics of silver can change in response to changing silver particle size and thus, it is plausible that more than one factor underlies the observed effects of particle size in ethylene epoxidation.

4. Conclusions

Particle size effects in Cl-promoted ethylene epoxidation over $Ag/\alpha\text{-}Al_2O_3$ catalysts reflect in part the underlying changes in chlorine coverage with particle size. Small particles are completely chlorided and plausibly act as Cl reservoirs resulting in low ethylene epoxidation rates over these particles while large particles have sub-monolayer Cl coverages, and it is these particles that catalyze ethylene epoxidation with high rates and high EO selectivity. Changes in chlorine coverage with particle size explain the shift in optimum average particle size that maximizes EO rates at different chlorinating conditions. These findings and their implications for EO catalysis were made possible by acknowledging the role of Cl content on the catalyst surface eschewing descriptions of Cl promotion only in terms of concentration of organochloride promoters in the gas phase.

CRediT authorship contribution statement

Krishna R. Iyer: Writing – review & editing, Writing – original draft, Investigation, Conceptualization. **Aditya Bhan:** Writing – review & editing, Supervision, Funding acquisition, Conceptualization.

Declaration of competing interest

The authors declare that they have no known competing financial interests or personal relationships that could have appeared to influence the work reported in this paper.

Data availability

Data will be made available on request.

Acknowledgements

Parts of this work were carried out in the Characterization Facility, University of Minnesota, which receives partial support from the NSF through the MRSEC and the NNCI programs. The authors acknowledge Mr. Michael Gresh-Sill and Mr. Joseph Esposito for acquiring chlorine uptake data on the $\alpha\text{-}Al_2O_3$ sample and for helpful technical discussions. We also acknowledge Drs. Christopher Ho, Victor Sussman, and Daniel Hickman at Dow Inc., for assistance with parameter estimation in Athena Visual and for helpful technical discussions. The authors gratefully acknowledge funding support from Dow through the University Partnership Initiative.

Appendix A. Supplementary material

Supplementary data to this article can be found online at https://doi.org/10.1016/j.jcat.2024.115583.

References

[1] T. Pu, H. Tian, M.E. Ford, S. Rangarajan, I.E. Wachs, Overview of selective oxidation of ethylene to ethylene oxide by Ag catalysts, ACS Catal. 9 (2019) 10727–10750, https://doi.org/10.1021/acscatal.9b03443.
[2] M.O. Ozbek, I. Onal, R.A. Van Santen, Why silver is the unique catalyst for ethylene epoxidation, J. Catal. 284 (2011) 230–235, https://doi.org/10.1016/j.jcat.2011.08.004.
[3] J.W. Harris, A. Bhan, Moderation of chlorine coverage and ethylene epoxidation kinetics via ethane oxychlorination over promoted $Ag/\alpha\text{-}Al_2O_3$, J. Catal. 367 (2018) 62–71, https://doi.org/10.1016/j.jcat.2018.08.021.
[4] K.R. Iyer, A. Bhan, Interdependencies among ethylene oxidation and chlorine moderation catalytic cycles over promoted $Ag/\alpha\text{-}Al_2O_3$ catalysts, ACS Catal. 11 (2021) 14864–14876, https://doi.org/10.1021/acscatal.1c03493.
[5] C.-J. Chen, J.W. Harris, A. Bhan, Kinetics of ethylene epoxidation on a promoted $Ag/\alpha\text{-}Al_2O_3$ catalyst-the effects of product and chloride co-feeds on rates and selectivity, Chem. Eur. J. 24 (2018) 12405–12415, https://doi.org/10.1002/chem.201801356.
[6] H. Shibata, A.G. Basrur, S. Gopal, M.H. McAdon, A.C.Y. Liu, L. Zhang, E.R. Frank, Method of formulating alkylene oxide catalyst in relation to catalyst reference properties, US9908861B2, (2018).
[7] K.R. Iyer, A. Bhan, Particle size dependence of ethylene epoxidation rates on $Ag/\alpha\text{-}Al_2O_3$ catalysts: why particle size distributions matter, J. Catal. 420 (2023) 99–109, https://doi.org/10.1016/j.jcat.2023.02.008.
[8] C. Campbell, The selective epoxidation of ethylene catalyzed by Ag(111): A comparison with Ag(110), J. Catal. 94 (1985) 436–444, https://doi.org/10.1016/0021-9517(85)90208-8.
[9] D.V. Demidov, I.P. Prosvirin, A.M. Sorokin, T. Rocha, A. Knop-Gericke, V. I. Bukhtiyarov, Preparation of Ag/HOPG model catalysts with a variable particle size and an in situ xps study of their catalytic properties in ethylene oxidation, Kinet. Catal. 52 (2011) 855–861, https://doi.org/10.1134/S002315841106005X.
[10] V.I. Bukhtiyarov, I.P. Prosvirin, R.I. Kvon, S.N. Goncharova, B.S. Bal'zhinimaev, XPS study of the size effect in ethene epoxidation on supported silver catalysts, J. Chem. Soc Faraday Trans. 93 (1997) 2323–2329, https://doi.org/10.1039/a608414a.
[11] G.N. Vayssilov, Y. Lykhach, A. Migani, T. Staudt, G.P. Petrova, N. Tsud, T. Skála, A. Bruix, F. Illas, K.C. Prince, V. Matolín, K.M. Neyman, J. Libuda, Support nanostructure boosts oxygen transfer to catalytically active platinum nanoparticles, Nat. Mater. 10 (2011) 310–315, https://doi.org/10.1038/nmat2976.
[12] L. Liu, A. Corma, Metal catalysts for heterogeneous catalysis: from single atoms to nanoclusters and nanoparticles, Chem. Rev. 118 (2018) 4981–5079, https://doi.org/10.1021/acs.chemrev.7b00776.
[13] W.S. Epling, G.B. Hoflund, D.M. Minahan, Study of Cs-promoted, α-alumina-supported silver, ethylene-epoxidation catalysts, J. Catal. 171 (1997) 490–497, https://doi.org/10.1006/jcat.1997.1831.
[14] P. Christopher, S. Linic, Shape- and size-specific chemistry of Ag nanostructures in catalytic ethylene epoxidation, ChemCatChem 2 (2010) 78–83, https://doi.org/10.1002/cctc.200900231.
[15] D.A. Hickman, J.C. Degenstein, F.H. Ribeiro, Fundamental principles of laboratory fixed bed reactor design, Curr. Opin. Chem. Eng. 13 (2016) 1–9, https://doi.org/10.1016/j.coche.2016.07.002.
[16] A.J.F. van Hoof, I.A.W. Filot, H. Friedrich, E.J.M. Hensen, Reversible restructuring of silver particles during ethylene epoxidation, ACS Catal. 8 (2018) 11794–11800, https://doi.org/10.1021/acscatal.8b03331.
[17] J.W. Harris, J.A. Herron, J.F. DeWilde, A. Bhan, Molecular characteristics governing chlorine deposition and removal on promoted Ag catalysts during ethylene epoxidation, J. Catal. 377 (2019) 378–388, https://doi.org/10.1016/j.jcat.2019.07.043.
[18] A.J.F. van Hoof, R.C.J. van der Poll, H. Friedrich, E.J.M. Hensen, Dynamics of silver particles during ethylene epoxidation, Appl. Catal. b: Env. 272 (2020) 118983, https://doi.org/10.1016/j.apcatb.2020.118983.
[19] C.T. Campbell, M.T. Paffett, The role of chlorine promoters in catalytic ethylene epoxidation over the Ag(110) surface, Appl. Surf. Sci. 19 (1984) 28–42, https://doi.org/10.1016/0378-5963(84)90051-5.
[20] M. Bowker, K.C. Waugh, Chlorine adsorption and chloridation of Ag(110), Surf. Sci. 155 (1985) 1–14, https://doi.org/10.1016/0039-6028(85)90399-1.
[21] M. Lamoth, T. Jones, M. Plodinec, A. Machoke, S. Wrabetz, M. Krämer, A. Karpov, F. Rosowski, S. Piccinin, R. Schlögl, E. Frei, Nanocatalysts unravel the selective state of Ag, ChemCatChem 12 (2020) 2977–2988, https://doi.org/10.1002/cctc.202000035.

[22] D. Chaparro, E. Goudeli, Oxidation rate and crystallinity dynamics of silver nanoparticles at high temperatures, J. Phys. Chem. C 127 (2023) 13389–13397, https://doi.org/10.1021/acs.jpcc.3c03163.
[23] L. Petrov, A. Eliyas, D. Shopov, Kinetics of ethylene oxidation over a silver catalyst in the presence of dichloroethane, Appl. Catal. 24 (1986) 145–161, https://doi.org/10.1016/S0166-9834(00)81264-6.
[24] V.I. Bukhtiyarov, A.F. Carley, L.A. Dollard, M.W. Roberts, XPS study of oxygen adsorption on supported silver: effect of particle size, Surf. Sci. 381 (1997) L605–L608, https://doi.org/10.1016/S0039-6028(97)00057-5.